Noname manuscript No.
(will be inserted by the editor)

Measuring Network Reliability and Repairability against Cascading Failures

Manish Thapa · Jose Espejo-Uribe · Evangelos Pournaras

Received: date / Accepted: date

Abstract Cascading failures on techno-socio-economic systems can have dramatic and catastrophic implications in society. A damage caused by a cascading failure, such as a power blackout, is complex to predict, understand, prevent and mitigate as such complex phenomena are usually a result of an interplay between structural and functional non-linear dynamics. Therefore, systematic and generic measurements of network reliability and repairability against cascading failures is of a paramount importance to build a more sustainable and resilient society. This paper contributes a probabilistic framework for measuring network reliability and repairability against cascading failures. In contrast to related work, the framework is designed on the basis that network reliability is multifaceted and therefore a single metric cannot adequately characterize it. The concept of 'repairability envelope' is introduced that illustrates trajectories of performance improvement and trade-offs for countermeasures against cascading failures. The framework is illustrated via four model-independent and application-independent metrics that characterize the topological damage, the network spread of the cascading failure, the evolution of its propagation, the correlation of different cascading failure outbreaks and other aspects by using probability density functions and cumulative distribution functions. The applicability of the framework is experimentally evaluated in a theoretical model of damage spread and an empirical one of power cascading failures. It is shown that the reliability and repairability in two systems of a totally different nature undergoing cascading failures can be better understood by the same generic measurements of the proposed framework.

Keywords cascading failure · metric · reliability · repairability · network · smart grid · disaster spread · repairability envelope

Manish Thapa · Jose Espejo-Uribe · Evangelos Pournaras
Professorship of Computational Social Science
ETH Zurich
Clausiusstrasse 50
Zurich, 8092
Switzerland
Tel.: +41 (0)44 63 20458
E-mail: {mthapa,josee,epournaras}@ethz.ch

1 Introduction

Cascading failures in techno-socio-economic infrastructures such as power grids, water/gas networks, economic markets, traffic systems and other critical infrastructures are the cause of massive social disruption and unrest, especially when their cause may be a result of targeted cyber attacks[1]. Their cost can be supreme for a society to afford, for instance, a 2003 power blackout in Canada has estimated costs of $4-$10 billions, with 50 millions of people left without electricity for up to 4 days (Liscouski and Elliot, 2004). Cascading failures are often a result of non-linear dynamics in which the interplay between structural and functional elements of a network is highly complex and challenging to measure. Given that the introduction of Internet of Things and pervasive computing in large-scale critical infrastructures brings unprecedented opportunities for online automated control, advanced measurements of cascading failures turns out to be of paramount importance. This paper introduces a framework for generic, yet highly empirical measurements of cascading failures that can characterize the system reliability as well as repairability when preventive or mitigation strategies are employed against cascading failures (Pournaras et al, 2013).

[1] For instance, US government claims that cyber attacks are the cause of power outages in Ukraine in 2015: https://ics-cert.us-cert.gov/alerts/IR-ALERT-H-16-056-01 (last accessed: December 2016)

The proposed evaluation framework is based on probabilistic measurements that characterize the overall network reliability and repairability of a system using probability density functions and cumulative distribution functions computed from empirical data. The overall network characterization is achieved by evaluating cascading failures triggered by every possible node or link failure, however, the analysis can be customized to more targeted link failures given the availability of empirical data (Ren et al, 2013; Dobson et al, 2007; Nedic et al, 2006) or other models studied in related work (Wang et al, 2015; Wang and Chen, 2008; Dobson et al, 2010). The framework is studied and illustrated by demonstrating four metrics that capture both topological and functional aspects of several flow networks: (i) *damage spread*, (ii) *cascade*, (iii) *spectral radius* and (iv) *damage correlation*. The framework does not exclude other relevant measures, however, this paper shows how these four metrics can provide a multifaceted indicator of reliability that is application-independent. Moreover, this paper studies the relevance of the proposed framework in measurements of repairability scenarios that have a preventive or mitigation role against cascading failures. The concept of the *repairability envelope* is introduced that defines for a certain preventive or mitigation action trajectories of performance improvement or performance trade-offs. The framework is evaluated by illustrating its applicability in two application scenarios, one in a theoretical model for disaster spread and one in an empirical model for power cascading failures. It is shown how the same measurements can characterize the overall system reliability and repairability in systems with highly diverse dynamics.

The contributions of this paper are the following:

- A generic probabilistic measurement framework of flow networks for a multifaceted characterization of network reliability under cascading failures.
- The concept of repairability envelope that defines the performance improvement and performance trade-offs when preventive or mitigation strategies against cascading failures are employed.
- An expanded evaluation methodology based on the proposed framework that provides new insights on earlier work (Buzna et al, 2007; Pournaras and Espejo-Uribe, 2016).

This paper is outlined as follows: Section 2 introduces the proposed measurement framework of cascading failures. Section 3 studies the applicability and experimentally evaluates the proposed framework in a theoretical model of disaster spread and an empirical model of power cascading failures. Section 4 compares the measurement framework with related work. Finally, Section 5 concludes this paper and outlines future work.

2 Measuring Cascading Failures

Table 1 illustrates the mathematical symbols used for the rest of this section in the order they appear. Assume a flow network of n nodes and l links represented by a directed weighted graph. Each node or link i in the network has a flow f_i and a capacity c_i. A cascading failure refers to consecutive overflows $f_i > c_i$ as a result (i) of an initial perturbation in the flow of the network and (ii) T redistributions of flow occurring over the directed links of the network. A flow perturbation refer to the removal of one or more nodes/links, the rewiring of a link, or changes in the flow of one or more nodes/links. The redistributions of the flow are referred to as *cascade iterations*.

This paper focuses on the $m-1$ contingency analysis as the perturbation model of cascading failures, where m is defined as follows:

$$m = \begin{cases} n & \text{if cascade over nodes} \\ l & \text{if cascade over links} \end{cases} \tag{1}$$

This model repeats the following process: a node or link is removed, the network undergoes a cascading failure, network performance is measured at every cascade iteration, the network is restored to its initial state and the whole process repeats for all m node or link removals. This model characterizes probabilistically the overall network reliability and repairability for a broad spectrum of stochastic perturbations. Moreover, an $m-1$ contingency analysis can be parallelized and efficiently computed in a fully distributed fashion, as well as in real-time if networks are not too large or computational resources not too limited (Balasubramaniam et al, 2013; Qin, 2015; Pournaras and Espejo-Uribe, 2016). The model can be extended to $m-x$ contingency analysis, which however has a higher computational complexity (Huang et al, 2009). Targeted attacks can also be computed via the $m-1$ contingency analysis by assigning failure probabilities to each node or link removal. Such probabilities can be computed using empirical data (Ren et al, 2013; Dobson et al, 2007; Nedic et al, 2006).

2.1 Network Reliability and Repairability

The concepts of network reliability and repairability are multifaceted and therefore, this paper claims that a single metric cannot capture the dynamics of different application domains. Thus, the reliability and repairability of a network against cascading failures, studied with the $m-1$ contingency analysis model, are measured by a sequence of met-

Table 1 An overview of the mathematical symbols

Symbol	Interpretation
n	Number of nodes
l	Number of links
i	An element: node or link
f_i	The flow of a node or link i
c_i	The capacity of a node or link i
T	Number of cascade iterations
m	Number of network elements: nodes or links
u	Metric index
t	Cascade iteration index
R	Reliability
$v_{u,i,t}$	Value of reliability metric u at cascade iteration t after element removal i
o	Number of metrics measuring reliability and repairability
$\hat{R}$	Network repairability
$\hat{v}_{u,i,t,j}$	Value of reliability metric u at cascade iteration t after element removal i with configuration j
$f_{u,t}(x)$	Probability density function for reliability using metric u at cascade iteration t
$f_{u,i}(x)$	Probability density function for reliability using metric u after element removal i
$\hat{f}_{u,t,j}(x)$	Probability density function for repairability using metric u at cascade iteration t with configuration j
$\hat{f}_{u,i,j}(x)$	Probability density function for repairability using metric u after element removal i with configuration j
$F_{u,t}(x)$	Cumulative distribution function for reliability using metric u at cascade iteration t
$F_{u,i}(x)$	Cumulative distribution function for reliability using metric u after element removal i
$\hat{F}_{u,t,j}(x)$	Cumulative distribution function for repairability using metric u at cascade iteration t with configuration j
$\hat{F}_{u,i,j}(x)$	Cumulative distribution function for repairability using metric u after element removal i with configuration j
$\hat{m}$	Number of survived nodes or links after a cascading failure
$p_{i,t}$	Probability to progress to the cascade iteration t after element removal i
$A_{i,t}$	Network adjacency matrix after element removal i at cascade iteration t
$\rho(A_{i,t})$	Spectral radius after element removal i at cascade iteration t
λ_n	The nth eigenvalue of the adjacency matrix
r_{xy}	Pearson correlation coefficient

rics, where each metric u is measured after the removal of node/link i at the tth cascade iteration:

$$\begin{aligned} R = v_{u,i,t}, \\ &\forall t \in \{1,...,T_i\}, \\ &\forall i \in \{1,...,m\} \text{ and} \\ &\forall u \in \{1,...,o\}, \end{aligned} \tag{2}$$

where T_i is the number of cascade iterations for the removal of node/link i, m is the number of each individual node or link removal for the $m-1$ contingency analysis and o is the number of metrics that characterize network reliability. Network repairability $\hat{R}$ refers to the increase of reliability R using preventive and mitigation strategies against cascading failures. It is measured as follows:

$$\begin{aligned} \hat{R} = \hat{v}_{u,i,t,j} - v_{u,i,t}, \\ &\forall t \in \{1,...,T_i\}, \\ &\forall i \in \{1,...,m\}, \\ &\forall u \in \{1,...,o\} \text{ and} \\ &\forall j \in \{1,...,k\}, \end{aligned} \tag{3}$$

where $\hat{v}_{u,i,t,j}, \forall t \in \{1,...,T_i\}, \forall i \in \{1,...,m\}, \forall u \in \{1,...,o\}$ and $\forall j \in \{1,...,k\}$ is the reliability of the network when preventive and mitigation strategies are employed. The additional dimension $j \in \{1,..,k\}$ is the number of configurations in which a preventive or mitigation strategy can operate. A configuration may represent a parameter tuning for improving performance or making a trade-off. The values of the metrics for all configurations form the *envelope of repairability*.

Given these fine grained measurements, the reliability and repairability can be illustrated with the following probability density functions:

$$f_{u,t}(x) = P(v_{u,t} = x),\ f_{u,i}(x) = P(v_{u,i} = x), \tag{4}$$

$$\hat{f}_{u,t,j}(x) = P(\hat{v}_{u,t,j} = x),\ \hat{f}_{u,i,j}(x) = P(\hat{v}_{u,i,j} = x), \tag{5}$$

where the probability density functions can be computed using the measurements of the $m-1$ contingency analysis for a certain cascade iteration t, or using the measurements of the cascade iterations for a certain node/line removal i. Alternatively, a formulation with the cumulative distribution function can be given as follows:

$$F_{u,t}(x) = P(v_{u,t} \leq x),\ F_{u,t}(x) = P(v_{u,t} \leq x), \tag{6}$$

$$\hat{F}_{u,t,j}(x) = P(\hat{v}_{u,t,j} \leq x),\ \hat{F}_{u,i,j}(x) = P(\hat{v}_{u,i,j} \leq x), \tag{7}$$

The rest of this section illustrates four metrics that can be included in the aforementioned expressions to characterize the reliability and repairability of several real-world complex networked systems.

2.2 Metrics

This paper illustrates four metrics for measuring network reliability and repairability under cascading failures: (i) *damage spread*, (ii) *cascade*, (iii) *spectral radius* and (iv) *damage correlation*. Although several other metrics (Yan et al, 2014; Mazauric et al, 2013; Youssef et al, 2011; Wang et al, 2015) can be used, this paper focuses on the aforementioned four ones that are model-independent and cover both topological and flow dynamics in networks undergoing cascading failures.

2.2.1 Damage spread

This metric concerns the probability of decreasing the percentage of remaining nodes or links, the nodes or links *survivability*, over the iterations of the cascade. It is defined as follows:

$$v_{1,t} = \sum_{x} F_{1,t}(x)\Delta x - \sum_{x} F_{1,t-1}(x)\Delta x, \tag{8}$$

where x represents the nodes or links survivability $\frac{\hat{m}_i}{m}$ with $\hat{m}_i \leq m$ the number of nodes or links survived after removal of node or link i. Δx is the integration step of the cumulative distribution function over the iterations of the cascading failure.

2.2.2 Cascade

This metric concerns the probability of advancing the iteration of a cascading failure. It is defined as follows:

$$v_{2,t} = \frac{1}{m}\sum_{i=1}^{m} p_{i,t}, \tag{9}$$

where:

$$p_{i,t} = \begin{cases} 1 & \text{if cascade progresses to } t \\ 0 & \text{otherwise} \end{cases} \tag{10}$$

represents the progress or not of the cascade to the next iteration after the removal of node or link i.

2.2.3 Spectral radius

This is a graph spectral metric calculated by the largest eigenvalue of the adjacency matrix $A_{i,t}$ of the network: $\rho(A_{i,t}) = \max\{|\lambda_1|, ..., |\lambda_{n_i}|\}$. By performing an $n-1$ contingency analysis, the spectral radius can be illustrated by the cumulative distribution function as follows:

$$v_{3,t} = F_{3,t}(x), \tag{11}$$

where x are the values of the $\rho(A_{i,t})$ for each removal of node i. Note that the measurements of the spectral radius can be also expressed with the area increase or decrease of the cumulative distribution function as expressed in Equation (8) for the damage spread:

$$v_{3,t} = \sum_{x} F_{3,t}(x)\Delta x - \sum_{x} F_{3,t-1}(x)\Delta x, \tag{12}$$

2.2.4 Damage correlation

Damage correlation computes the Pearson correlation coefficient r_{xy} between two vectors x and y of node or link values:

$$v_{4,t} = r_{xy}, \tag{13}$$

where the vectors represent the status of the network after a node or link removal i and j respectively. Several relevant metrics for nodes and links can be used to measure the values of the vectors, for example, a binary variable denoting if the nodes or links fail during a cascading failure or the ratio $\frac{f_i}{c_i}$ that denotes the utilization of the nodes or links.

3 Applicability and Experimental Evaluation

The proposed measurement framework is evaluated on the basis of two illustrations: (i) The applicability of the cascading failure measurements in two use cases, one in a theoretical state-of-the-art model (Buzna et al, 2007) of disaster spread and one in the application domain of power networks (Pournaras and Espejo-Uribe, 2016). (ii) Quantitative results on reliability and repairability for each of the two use cases. The goal of this section is to make a proof-of-concept and inspire community to expand the proposed framework with new reliability and repairability metrics as well as further use cases. The results illustrated in this paper are new and they are not shown in the primary earlier work of the two use cases. The measurements shown in this section are agnostic and independent of the two very different use cases, in contrast to the primary earlier work in which model-dependent measurements are performed.

The proposed framework[2] is implemented using the SFINA framework[3], the *Simulation Framework for Intelligent Network Adaptations* (Pournaras et al, 2017). Experiments ran on a MacBook Pro, 2.3 GHz Intel Core i5 with 4 GB RAM. Cascading failures are visualized with an implemented integration[4] of Gephi in SFINA. In this paper, 'baseline'

[2] Available at `https://github.com/SFINA/Flow-Monitor` (last accessed: December 2016)

[3] Available at `https://github.com/SFINA` (last accessed: December 2016)

[4] Available at `http://gephi.github.io` (last accessed: December 2016)

refers to the networks undergoing cascading failures without any repairability strategy applied.

3.1 Theoretical model: disaster spread

The theoretical model for disaster spread is evaluated on two artificial networks: (i) *Barabási-Albert* and (ii) *small world*. The two networks have 100 nodes and 100 bidirectional links. The Barabási-Albert network is built with a probability of 0.15 that a new node added is connected to an existing node. The small world network is built with a rewiring probability of 0.15 and mean degree of 3.

According to the damage spread model, each node calculates a set of coupled differential equations. Each equation governs the change of 'damage' in a node over time. Each node is characterized by a *damage level* and a *tolerance threshold* θ with an α *gain parameter* over which the node is fully damaged. Moreover, each node has a *recovery rate* τ_{start} and the spread of the damage in interconnected nodes is a function of the node degree. Each link is characterized by the *connection strength*, a *time delay* t_{ij} and the β *parameter* that models the physical characteristics of the surrounding. The *a* and *b fit parameters* weight the influence of node degree on the disaster spread process. More information about the mathematical model and its parameters is out of the scope of this paper. They are defined in detail in Equation (2) of the earlier work (Buzna et al, 2007).

The $m-1$ contingency analysis introduces a damage level of 4.0 in a node and repeats the process for all nodes. The parameters of the model are illustrated here for the repeatability of results. Node parameters are chosen as $\alpha = 5$, $\beta = 0.025$, $\theta = 0.5$ and $\tau_{start} = 4$. Link parameters are chosen as a connection strength of 0.5, t_{ij} from a χ^2 distribution with $\mu = 4$, a scaling factor of 0.05 and a translation factor of 1.2. Moreover, it is set $a = 4$ and $b = 3$. Two repairability strategies[5] are employed from the earlier published work: (i) *strategy A* and (ii) *strategy B*. The strategies are implemented as SFINA applications by extending the simulation agent so that they can be reused by other disaster spread models in the future. This flexibility is the result of the generic and modular design of SFINA Pournaras et al (2017). The strategies define resources for recovery from a resource distribution function $r(t) = a_1 t^{b_1} e^{-c_1 t}$, with $a_1 = 10$, $b_1 = 0.5$ and $c_1 = 0.03$. Parameter a_1 is the one varied to compute the envelope of repairability. The equation and parameters model an initial exponential increase and a gradual decay of resources over time. Resources are supplied after the 10th simulation step. Finally, the recovery rate of a node at a specified time is given by $1/\tau_i(t) = 1/(\tau_{start} - \beta_2)e^{-\alpha_2 R_i(t)} + \beta_2$ with $\alpha_2 = 0.58$ and $\beta_2 = 0.2$. These parameters are evaluated earlier to give an efficient response to disaster spread.

[5] These strategies correspond to the strategy 3 and 4 in the earlier work (Buzna et al, 2007)

Figure 1 illustrates the likelihood of damage spread for the two artificial networks. In the Barabási-Albert network of Figure 1a, the two repairability strategies decrease the overall damage spread by 8.7% and 9.1% respectively, however, the damage spreads rapidly over the hub nodes of the network. The damage increasingly spreads during the first 20 iterations, while at the later cascade iterations the recovery process minimizes the spread. On the other hand, the small world network of Figure 1b has lower levels of damage spread with the strategies providing a higher repairability compared to the Barabási-Albert network: 17.5% and 34.4% respectively.

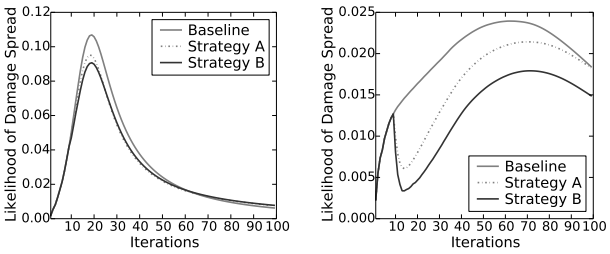

(a) BarabásiAlbert network (b) Small world network

Fig. 1 Likelihood of damage spread for the two artificial networks using strategy A and B.

The damage spread and damage correlation measurements are validated quantitatively and qualitatively in Appendix B for a Barabási-Albert and a small world network.

In case the resources available for the recovery can increase using higher values of a_1, the envelope of self-repairability is formed according to Figure 2. The Barabási-Albert network of Figure 2a has a broadening envelope as damage spread increases and a narrowing envelope as the damage spread decreases. The same holds for the small world network of Figure 2b that has overall broader envelope even if lower values of the a_1 parameter are used.

In contrast to the evaluation methodology illustrated in the original earlier work (Buzna et al, 2007), the reliability and repairability of two different artificial networks with different settings are illustrated without measuring model-specific parameters but rather generic metrics that equip the proposed framework. The rest of this section illustrates how the same metrics can characterize the reliability and repairability in an empirical networked system of a totally different nature: power systems undergoing cascading failures and using smart transformers for system self-repair.

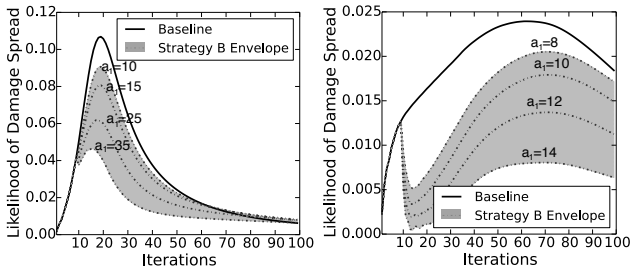

(a) Barabasi network (b) Small world network

Fig. 2 Repairability envelopes for the two artifical networks and strategy B by varying the parameter a_1.

3.2 Empirical model: power cascading failures

In the use case of power networks, three IEEE reference networks are used[6]: (i) *case-39*, (ii) *case-57*, (iii) *case-118* and (iv) *case-2383*. Case-39 has capacity information referred to as link rating, while the rest of the networks use the $\alpha = 2.0$ parameter that computes the link capacities based on the load profile of the networks. All power networks run AC power flow analysis except case-2383 that runs DC power flow analysis for faster performance and convergence. In all cases, the power flow analysis runs using the InterPSS[7] (Zhou and Zhou, 2007) SFINA backend.

The $m-1$ contingency analysis is applied by removing a link and repeating the process for all links. The simulation model of cascading failures is illustrated in earlier work (Pournaras and Espejo-Uribe, 2016) and it concerns redistribution of power flows after link failures caused by flows overpassing link capacities, the *line ratings*. For the repairability of the case-39 network against cascading failures, 5 coordinating smart transformers are introduced in a random placement[8]. The smart transformers control and collectively optimize the phase angle of the link they reside on to improve reliability (Pournaras and Espejo-Uribe, 2016). The envelope of repairability is computed by varying the penalty parameter λ of the optimization, with the default value being $\lambda = 1.0$. This parameter controls the penalization applied in the magnitude of change in the phase angle. Strategy B from earlier work (Pournaras and Espejo-Uribe, 2016) is used in the performed experiments.

Figure 3 illustrates the likelihood of damage spread and cascade in the three power networks. Case-57 has the highest disaster spread followed by case-118 and case-2383. It is evident that the size of the network plays a role here given that the $m-1$ contingency analysis always removes a single link. Line failures spread further in case-2383 with the highest size, however, the percentage of links affected is still lower than case-118 and case-57 that have a lower size.

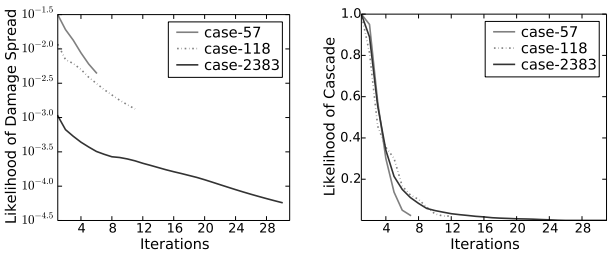

(a) Damage spread (b) Cascade

Fig. 3 Likelihood of damage spread and cascade for three networks under cascading failure.

The damage spread in Figure 3a is computed based on Equation (8). The original cumulative distribution functions for link survivability based on which Equation (8) is computed are illustrated in Figure 4a, 4c and 4e. For each of these plots, the respective plot for the spectral radius is shown as well. The plots show the evolution of the cascading failures by increasing probabilities values of the lower link survivability values at the later cascade iterations. The spectral radius shows a similar trend. Case-57 has lower values of spectral radius than case-118.

Figure 5 illustrates the damage correlation for case-57 and case-118. Due to the large network size, case-2383 does not show significant influence on damage correlation and therefore, results are not shown. The damage correlation map in case-57 remains similar during the evolution of the cascading failure. In contrast, the damage correlations of case-118 shift to different link pairs at the last iteration of the cascading failure.

Figure 6 illustrates the visualization of the two network at two different iterations of a cascading failure. The attacked link is indicated at iteration 1 with red color followed by several other red trimmed links at iteration 5 in case-47 and case-118.

Network repairability is applied by using coordinated smart transformers. Figure 7 shows the improvement in repairability. In Figure 7a, the likelihood of increasing damage spread is 37.5% lower when smart transformers are used. Figure 7b confirms that the cascading failure terminates at iteration 2 instead of iteration 6 thanks to smart transformers.

Figure 8 illustrates the evolution of the spectral radius with and without smart transformers. By mitigating cascading failures, the spectral radius remains at high values throughout the iterations of the cascading failure.

[6] Available at `http://www.pserc.cornell.edu/matpower/docs/ref/matpower5.0/menu5.0.html` (last accessed: December 2016)

[7] Available at `http://www.interpss.com` (last accessed: December 2016)

[8] Several such placements are evaluated in earlier work (Pournaras and Espejo-Uribe, 2016).

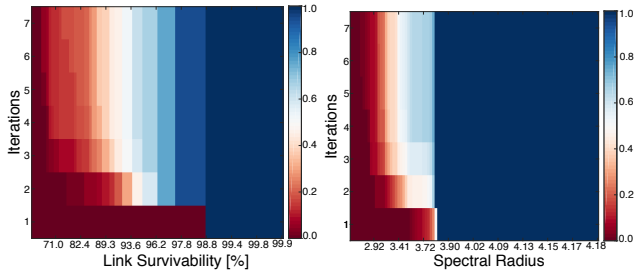

(a) Case-57, link survivability

(b) Case-57, spectral radius

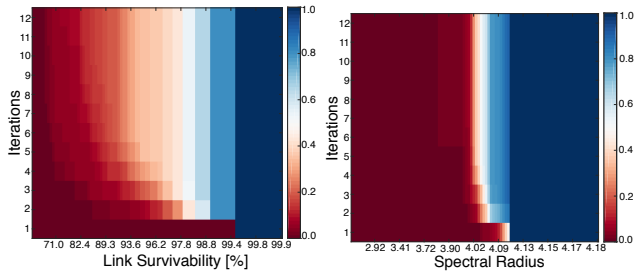

(c) Case-118, link survivability

(d) Case-118, spectral radius

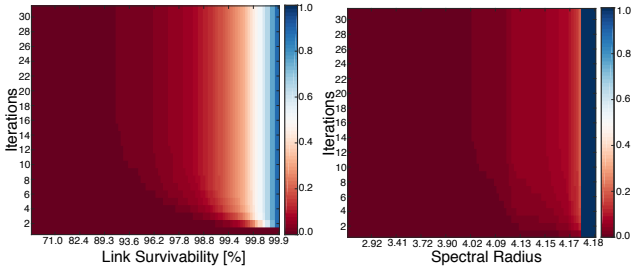

(e) Case-2383, link survivability

(f) Case-2383, spectral radius

Fig. 4 Evolution of the cumulative distribution functions of link survivability and spectral radius in three networks under cascading failure.

Figure 9 illustrates the damage correlation matrix. It is shown that the flow redistributions, which smart transformers perform create highly uncorrelated link failures. This is because each local control of the phase angle in a link results in a global flow redistribution in the optimization space that are in contrast to the default redistributions computed by the cascading failure model.

Figure 10 visualizes a cascading failure in case-39 without and with smart transformers. It is clearly shown that a fewer number of links are trimmed when smart transformers are used.

In this empirical scenario, computing the envelope of self-repairability is a way to visually evaluate parameter fitting for the optimization process that controls the phase angles of the smart transformers. For this purpose, different λ values are tested and aggregated to the envelope of Figure 11. It is confirmed that low values of the penalty parameter achieve higher repairability, which is a result of allowing higher magnitudes of changes on the phase angle.

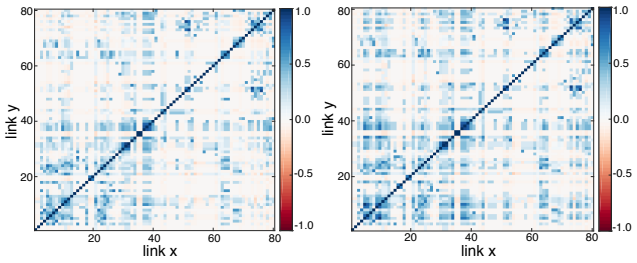

(a) Case-57, iteration 2

(b) Case-57, iteration 6

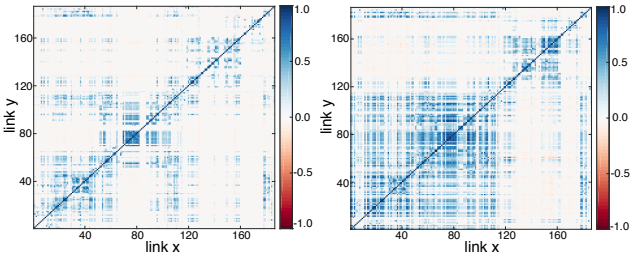

(c) Case-118, iteration 2

(d) Case-118, iteration 11

Fig. 5 Damage correlation in three networks under cascading failure.

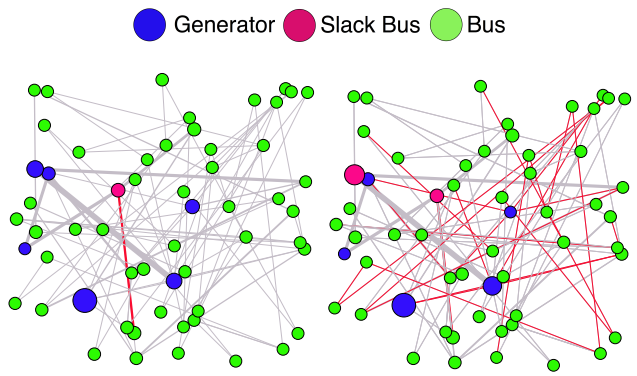

(a) Case-57, iteration 1

(b) Case-57, iteration 5

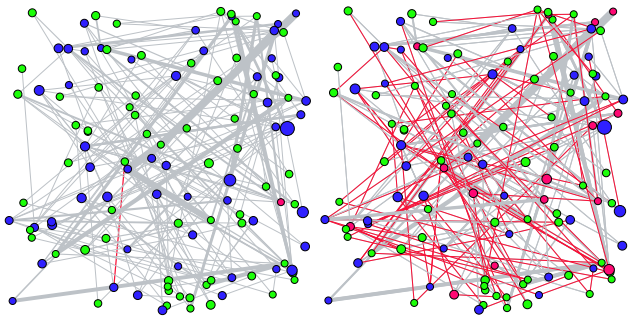

(c) Case-118, iteration 1

(d) Case-118, iteration 5

Fig. 6 Visualization of cascading failures in two networks. The size and thinkness of the lines is proportional to the power flows served. Trimmed links are indicated with red color. Generators inject power flows, slack buses balance power flows and buses transfer and consume them.

The applicability of the framework measurements in this empirical model of power cascading failures confirms its

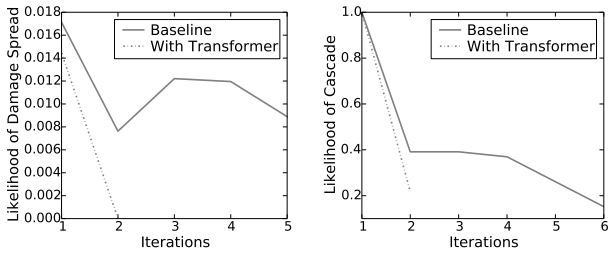

(a) Damage spread (b) Cascade

Fig. 7 Likelihood of damage spread and cascade in case-39 with and without smart transformers.

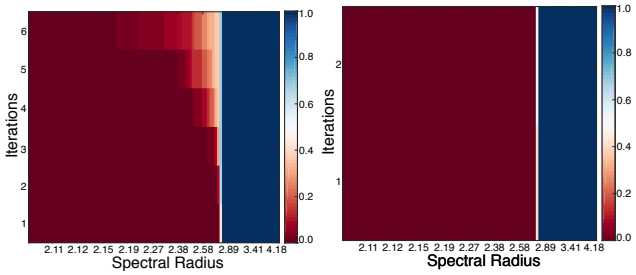

(a) Without smart transformers (b) With smart transformers

Fig. 8 Evolution of spectral radius in case-39 with and without smart transformers.

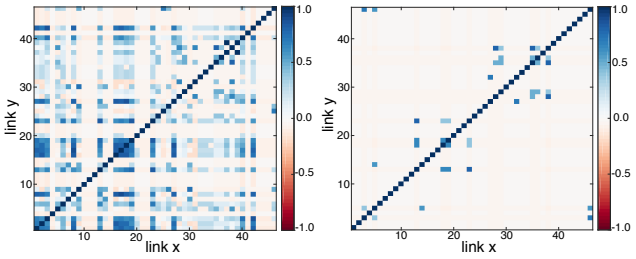

(a) Without smart transformers (b) With smart transformers

Fig. 9 Damage correlation in case-39 with and without smart transformers.

generic design and its flexibility to characterize the multi-faceted aspects of network reliability and repairability against cascading failures. Regardless of DC or AC power flows, the network type, the use of smart transformers for balancing flow distributions, or even the optimization applied for these flow redistributions, the same framework is capable of characterizing, as well as, comparing system reliability and repairability.

4 Comparison with Related Work

Several application-independent metrics are introduced in the research area of flow networks, which are applicable for use in the proposed framework, for instance through-

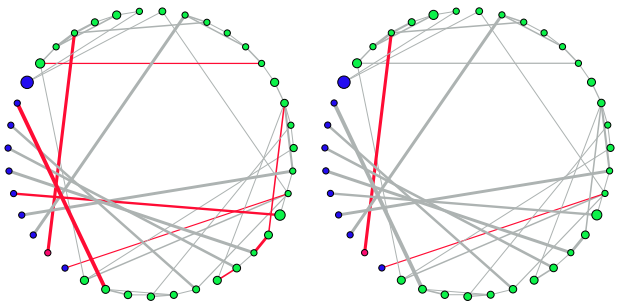

(a) Without smart transformers (b) With smart transformers

Fig. 10 Visualization of a cascading failure in case-39 without and with smart transformers.

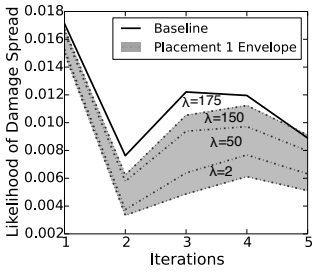

Fig. 11 Repairability envelope in case-39 without and with smart transformers of different λ parameter.

put (Todinov, 2013; Huseby and Natvig, 2013), however they have not been studied in the context of cascading failures. Other metrics such as the Birnbaums, BarlowProschan and the Natvig measures characterize the reliability of a network in respect to the failure or repair of an individual component. Kuo and Zhu (2012) classify importance measures in reliability into structure, reliability and lifetime types based on the knowledge that determines them. Given that the proposed framework focuses on the overall characterization of system reliability and repairability, such metrics are highly relevant when they measure global system properties rather than component reliability as well as they do not depend on a specific model or scenario. Moreover, note that the applicability of several of these metrics require fine-grained empirical data, for instance, repair and failure rates of individual components.

Metrics for measuring reliability against cascading failures are earlier introduced. Wang et al (2015) study cascading failures in power grids and introduce the normalized, to the load profile of the network, served power demand as a reliability measure. In contrast to this work, measurements for the evolution of the cascade are not studied and the attack model is based on the node significance centrality of a single link, whereas, the proposed framework pro-

vides an overall probabilistic estimation of reliability using the $m-1$ contingency analysis. This is also the case for the work of Zhang et al (2014) that measures the percentage of failures in the network and correlates complex networks with reliability measures. Cascading failures are triggered by random node selections or selections based on node degrees. No information about the evolution of the cascading failures is measured.

Wang and Chen (2008) introduce a robustness metric that models link weights based on the node degrees of the associated nodes. Cascading failures are triggered using the sandpile model by adding flows incrementally. Although this model can be used in analyses of how node degrees influence the reliability of flow networks, the use of empirical data shown in this work can provide more direct, accurate and model-independent calculations of reliability.

Dobson et al (2010) introduce a statistical estimator to quantify the propagation of cascading failures in power transmission lines. Their model relies on Poisson distribution for the propagation of failures, which may not hold for different flow network models, cascading processes or application domains. The networks evaluated are low in size and require parameter tuning, for instance the saturation parameter. In contrast, the measurements proposed in this paper are model-independent, therefore, they have a higher applicability.

Youssef et al (2011) illustrate a robustness measure for power grids with respect to cascading failures. This work draws several parallels with the work proposed in this paper, for instance, a probabilistic model for link survivals is shown. Moreover, the depth of the cascading failure is measured and links are ranked according to their failure probabilities under cascading failures. However, this earlier work is limited to DC power flows and it is mainly a topological analysis of the network, in contrast to the proposed framework that is illustrated for several application-independent metrics.

In respect to network repairability and related work on repairability envelopes illustrated in this paper, Trajanovski et al (2013) introduce robustness envelopes by computing approximate network performance probability density functions as functions of the fraction of nodes removed. The robustness envelopes and targeted attack responses are computed by network rewiring to increase or decrease degree assortativity. This is mainly a topological and graph spectral analysis, in contrast to the envelopes of this work that capture functional aspects of the network operations and repair mechanisms. Ulanowicz et al (2009) introduce the concept of 'window of vitality' that circumscribes sustainable behavior in ecosystems. The window of vitality is studied in the context of biological ecosystems, however, the concept could be used to heuristically show how different networks and configurations are reliable given different scenarios.

5 Conclusion and Future Work

This paper concludes that the proposed measurement framework is generic and can capture multifaceted aspects of network reliability, as well as repairability, in complex systems undergoing cascading failures. This is shown by the applicability of the framework and extensive measurements in a theoretical model of disaster spread and an empirical model of power cascading failures. It is shown that the same measurements can provide new insights about system reliability and repairability as well as a better understanding on the evolution of cascading failures in several networks. This comes in contrast to related work in which measurements do not capture the evolutionary aspects of cascading failures and are often tailored to the model under scrutiny or the application domain.

Future work includes the expansion of the framework with other probabilistic measurements and the evaluation of other attack models that use real-world empirical data on triggering cascading failures. The feasibility of the framework in real-time system operations for distributed monitoring and online automated decision-support is also subject of future work (Pournaras, 2013).

Acknowledgements This research is funded by the Professorship of Computational Social Science, ETH Zurich, Zurich, Switzerland. The authors are grateful to the rest of the SFINA development team for their comments and overall contributions to the project: Ben-Elias Brandt, Mark Ballandies and Dinesh Acharya.

References

Balasubramaniam K, Venayagamoorthy GK, Watson N (2013) Cellular neural network based situational awareness system for power grids. In: Neural Networks (IJCNN), The 2013 International Joint Conference on, IEEE, pp 1–8

Buzna L, Peters K, Ammoser H, Kühnert C, Helbing D (2007) Efficient response to cascading disaster spreading. Physical Review E 75(5):056,107

Dobson I, Carreras BA, Lynch VE, Newman DE (2007) Complex systems analysis of series of blackouts: Cascading failure, critical points, and self-organization. Chaos: An Interdisciplinary Journal of Nonlinear Science 17(2):026,103

Dobson I, Kim J, Wierzbicki KR (2010) Testing branching process estimators of cascading failure with data from a simulation of transmission line outages. Risk Analysis 30(4):650–662

Huang Z, Chen Y, Nieplocha J (2009) Massive contingency analysis with high performance computing. In: 2009 IEEE Power & Energy Society General Meeting, IEEE, pp 1–8

Huseby AB, Natvig B (2013) Discrete event simulation methods applied to advanced importance measures of repairable components in multistate network flow systems. Reliability Engineering & System Safety 119:186 – 198

Kuo W, Zhu X (2012) Some recent advances on importance measures in reliability. IEEE Transactions on Reliability 61(2):344–360

Liscouski B, Elliot W (2004) Final report on the august 14, 2003 blackout in the united states and canada: Causes and recommendations. A report to US Department of Energy 40(4)

Mazauric D, Soltan S, Zussman G (2013) Computational analysis of cascading failures in power networks. ACM SIGMETRICS Performance Evaluation Review 41(1):337–338

Nedic DP, Dobson I, Kirschen DS, Carreras BA, Lynch VE (2006) Criticality in a cascading failure blackout model. International Journal of Electrical Power & Energy Systems 28(9):627–633

Pournaras E (2013) Multi-level reconfigurable self-organization in overlay services. PhD thesis, TU Delft, Delft University of Technology

Pournaras E, Espejo-Uribe J (2016) Self-repairable smart grids via online coordination of smart transformers. IEEE Transactions on Industrial Informatics PP(99):1–1, (to appear)

Pournaras E, Yao M, Ambrosio R, Warnier M (2013) Organizational control reconfigurations for a robust smart power grid. In: Internet of Things and Intercooperative Computational Technologies for Collective Intelligence, Springer, pp 189–206

Pournaras E, Brandt BE, Thapa M, Acharya D, Espejo-Uribe J, Ballandies M, Helbing D (2017) Sfina - simulation framework for intelligent network adaptations. Simulation Modelling Practice and Theory (to appear)

Qin Z (2015) Construction of generic and adaptive restoration strategies. HKU Theses Online (HKUTO)

Ren H, Xiong J, Watts D, Zhao Y, et al (2013) Branching process based cascading failure probability analysis for a regional power grid in china with utility outage data. Energy and Power Engineering 5(04):914

Todinov MT (2013) Flow Networks: Analysis and optimization of repairable flow networks, networks with disturbed flows, static flow networks and reliability networks. Newnes

Trajanovski S, Martín-Hernández J, Winterbach W, Van Mieghem P (2013) Ulanowicz2009. Journal of Complex Networks 1(1):44–62

Ulanowicz RE, Goerner SJ, Lietaer B, Gomez R (2009) Quantifying sustainability: Resilience, efficiency and the return of information theory. Ecological Complexity 6(1):27 – 36

Wang WX, Chen G (2008) Universal robustness characteristic of weighted networks against cascading failure. Physical Review E 77(2):026,101

Wang X, Koç Y, Kooij RE, Van Mieghem P (2015) A network approach for power grid robustness against cascading failures. In: Reliable Networks Design and Modeling (RNDM), 2015 7th International Workshop on, IEEE, pp 208–214

Yan J, He H, Sun Y (2014) Integrated security analysis on cascading failure in complex networks. IEEE Transactions on Information Forensics and Security 9(3):451–463

Youssef M, Scoglio C, Pahwa S (2011) Robustness measure for power grids with respect to cascading failures. In: Proceedings of the 2011 International Workshop on Modeling, Analysis, and Control of Complex Networks, International Teletraffic Congress, pp 45–49

Zhang W, Pei W, Guo T (2014) An efficient method of robustness analysis for power grid under cascading failure. Safety Science 64:121–126

Zhou M, Zhou S (2007) Internet, open-source and power system simulation. In: Power Engineering Society General Meeting, 2007. IEEE, pp 1–5

A Theoretical Model: Damage Correlation

To better understand the spreading dynamics, the evolution of damage correlation for the two artificial networks is shown in Figure 12 and Figure 13. The two figures show how correlated the spreading of network damages are in all possible pairs of perturbations in the network and how the correlations evolve during the cascading failure.

Figure 12 confirms that the hubs of the Barabási-Albert network result in highly positively correlated processes of damage spread, which are actually due to the high levels of damage diffused in the network. When the recovery process takes place, there is a low increase in the average correlations for strategy B compared to baseline, for instance, 3.95% at the 30th cascade iteration compared to 0.5% at the 20th iteration.

Figure 13 confirms that the damage spread in small world networks has a strong locality influence. The damage of neighboring nodes results in correlated spread of damages as it can be clearer seen in Figure 13a, 13e and 13i. As the spread of the damage increases according the trajectories of Figure 1b, the correlation of the damages becomes more polarized and vary between highly positive and negative correlation in different parts of the network. Strategies decrease correlations compared to the baseline, for instance, 25.44% at the 30th cascade iteration and 41.5% at the 70th iteration for strategy B. However, damage correlations increase on average during the cascading failure, for example, 87% and 83.6% for baseline and strategy B respectively and from the 30th to the 70th iteration of the cascading failure.

B Theoretical Model: Network Visualizations

Figure 14 and Figure 15 show the two artificial networks in the respective cascade iterations that are also shown for the damage correlations. The initial damaged node is node 7.

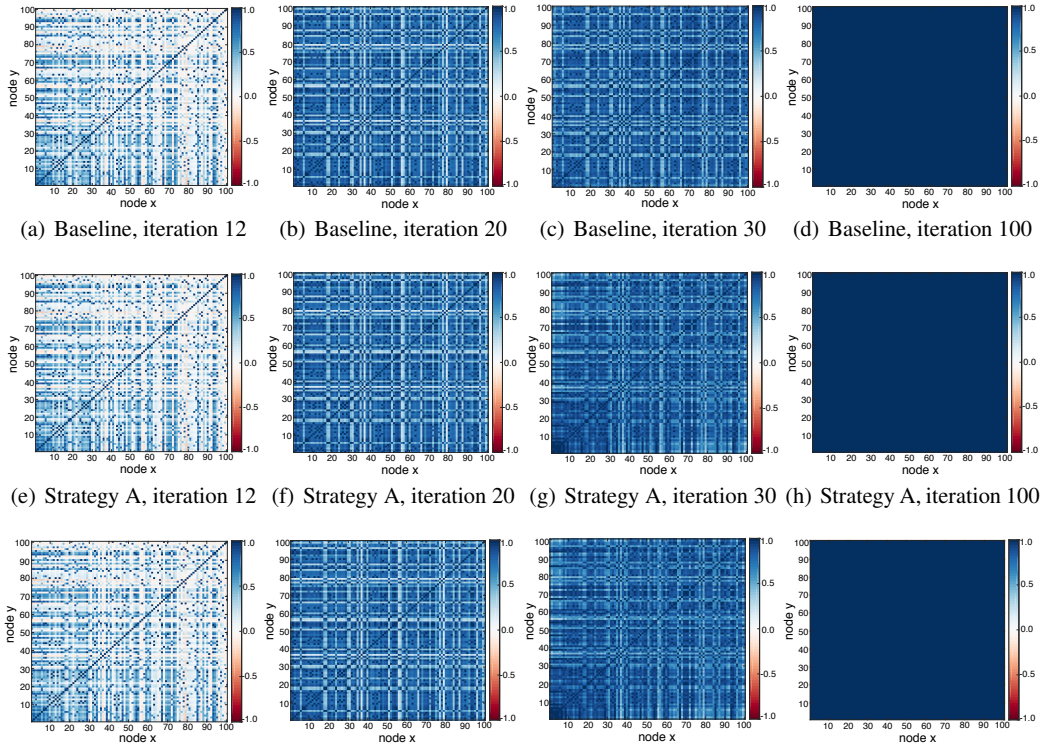

(a) Baseline, iteration 12 (b) Baseline, iteration 20 (c) Baseline, iteration 30 (d) Baseline, iteration 100

(e) Strategy A, iteration 12 (f) Strategy A, iteration 20 (g) Strategy A, iteration 30 (h) Strategy A, iteration 100

(i) Strategy B, iteration 12 (j) Strategy B, iteration 20 (k) Strategy B, iteration 30 (l) Strategy B, iteration 100

Fig. 12 Damage correlation in the Barabási-Albert network at different cascade iterations. (a)-(d) Baseline, (e)-(h) strategy A and (i)-(l) strategy B.

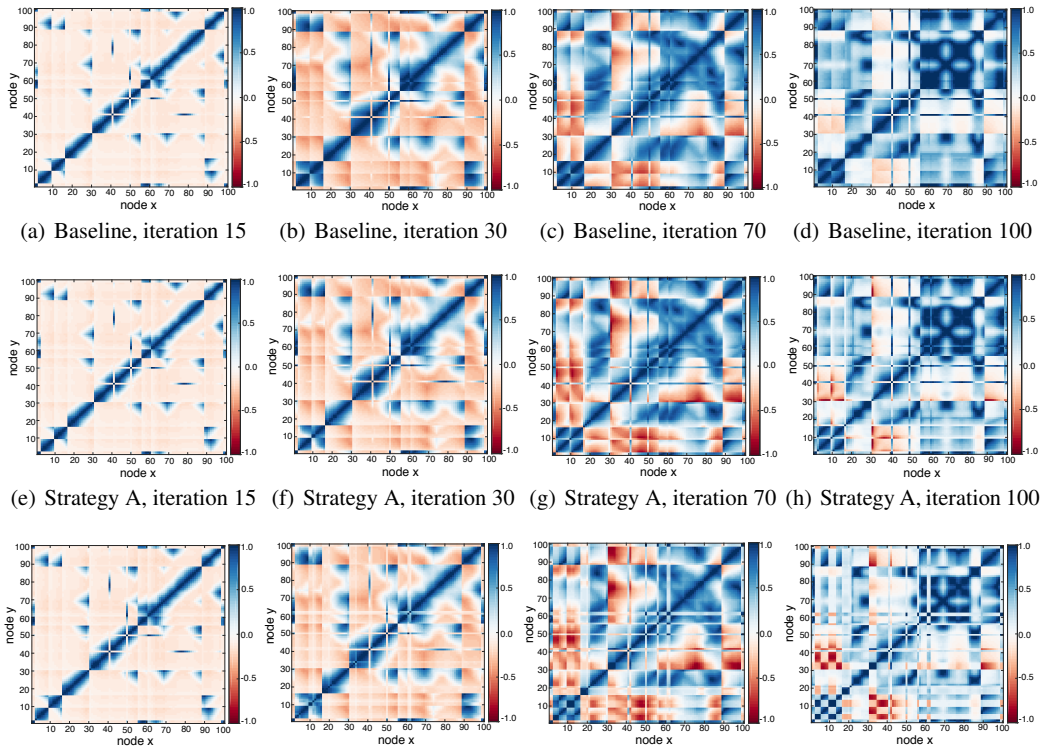

(a) Baseline, iteration 15 (b) Baseline, iteration 30 (c) Baseline, iteration 70 (d) Baseline, iteration 100

(e) Strategy A, iteration 15 (f) Strategy A, iteration 30 (g) Strategy A, iteration 70 (h) Strategy A, iteration 100

(i) Strategy B, iteration 15 (j) Strategy B, iteration 30 (k) Strategy B, iteration 70 (l) Strategy B, iteration 100

Fig. 13 Damage correlation in the small world network at different cascade iterations. (a)-(d) Baseline, (e)-(h) strategy A and (i)-(l) strategy B.

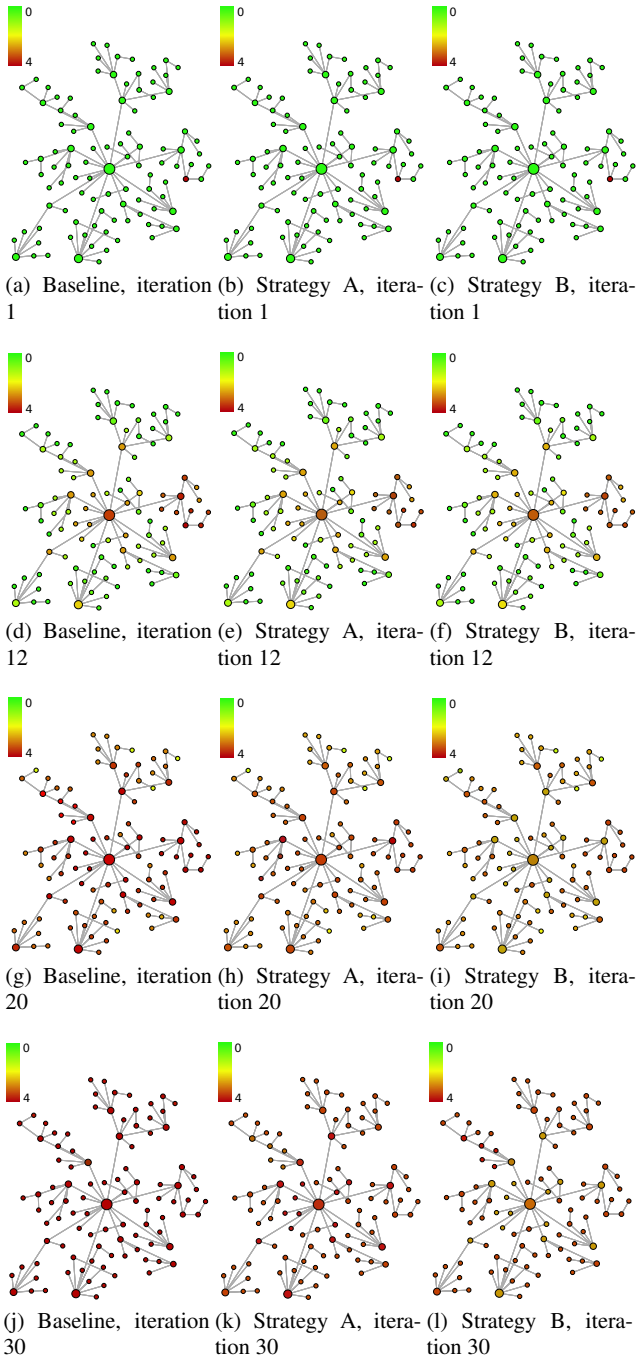

(a) Baseline, iteration 1 (b) Strategy A, iteration 1 (c) Strategy B, iteration 1

(d) Baseline, iteration 12 (e) Strategy A, iteration 12 (f) Strategy B, iteration 12

(g) Baseline, iteration 20 (h) Strategy A, iteration 20 (i) Strategy B, iteration 20

(j) Baseline, iteration 30 (k) Strategy A, iteration 30 (l) Strategy B, iteration 30

Fig. 14 Visualization of cascading failure in the Barabási-Albert network. (a), (d), (g), (j): Baseline, (b), (e), (h), (k) strategy A and (c), (f), (i), (l) strategy B. The pallete indicates the damage level of the nodes in the range $[0,4]$.

The Barabási-Albert network in Figure 14 clearly shows that the damage of the peripheral node influences the neighboring nodes (Figures 14d, 14f), however, as the central hub is only two hops away from the damaged node, the damage spreads and eventually affects severely the whole network already at the 20th iteration (Figures 14g, 14i). The repairability strategies can only alleviate the damage level of individual nodes and therefore, they do not restrict the cascading disaster.

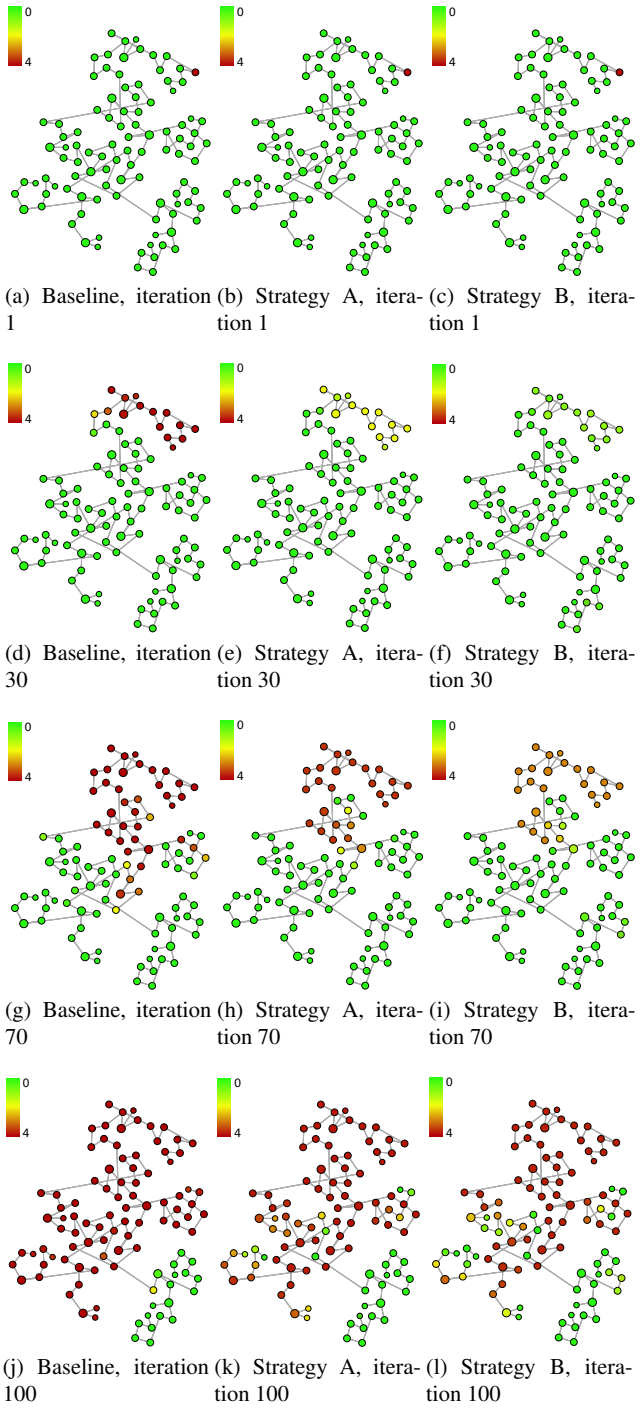

(a) Baseline, iteration 1 (b) Strategy A, iteration 1 (c) Strategy B, iteration 1

(d) Baseline, iteration 30 (e) Strategy A, iteration 30 (f) Strategy B, iteration 30

(g) Baseline, iteration 70 (h) Strategy A, iteration 70 (i) Strategy B, iteration 70

(j) Baseline, iteration 100 (k) Strategy A, iteration 100 (l) Strategy B, iteration 100

Fig. 15 Visualization of cascading failure in the small world network. (a), (d), (g), (j): Baseline, (b), (e), (h), (k) strategy A and (c), (f), (i), (l) strategy B. The pallete indicates the damage level of the nodes in the range $[0,4]$.

In contrast, the small world network of Figure 15 shows that the damage spread is in general localized at a higher level than the Barabási-Albert network. Strategy B maintains the lowest damage level in the nodes as also confirmed by Figure 1b.